



## The effects of tea plant age on the color, taste, and chemical characteristics of Yunnan Congou black tea by multi-spectral omics insight

Piaopiao Long<sup>a</sup>, Shengxiao Su<sup>a</sup>, Zisheng Han<sup>b</sup>, Daniel Granato<sup>c</sup>, Wei Hu<sup>a</sup>, Jiaping Ke<sup>a</sup>, Liang Zhang<sup>a,\*</sup>

<sup>a</sup> State Key Laboratory of Tea Plant Biology and Utilization, Anhui Agricultural University, Hefei, China

<sup>b</sup> Department of Food Science, Rutgers University, New Brunswick, NJ 08901, USA

<sup>c</sup> Bioactivity and Applications Laboratory, Department of Biological Sciences, University of Limerick, Limerick V94 T9PX, Ireland

### ARTICLE INFO

#### Keywords:

Black tea  
Color  
Taste  
Multi-spectral omics  
Amadori rearrangement product

### ABSTRACT

The present study comprehensively used integrated multi-spectral omics combined with sensory evaluation analysis to investigate the quality of three types of Yunnan Congou black teas from different tree ages (decades, DB; hundreds, HB; a thousand years, TB). TB infusion presented the highest scores of sweetness and umami, higher brightness, and yellow hue. Eighty-four marker metabolites were identified, including Amadori rearrangement products, catechin oxidation products, flavonoid glycosides, and organic acids, which are simultaneously related to tea infusions' color and taste. Moreover, the content of some characteristic flavonoid glycosides and organic acids was determined. Our finding implied *trans*-4-*O*-*p*-coumaroylquinic acid and quercetin 3-*O*-rutinoside contributed to bitterness and astringency, while dehydro theanine-glucose Amadori product and xylopyranosyl-glucofuranose resulted in umami and sweetness. These results provided quantitative and qualitative information for deciphering differences among black teas with different tea plant ages, conducting to the further utilization of ancient tea plants in Southwest China.

### 1. Introduction

Black tea is a type of tea that has been widely studied over decades due to its various health benefits and pleasant flavor characteristics (Kamiloglu et al., 2021). Its unique characteristics are mainly influenced by the quality of fresh leaves and the processing technologies applied (Zhu et al., 2020). According to variations in processing techniques, black tea categories mainly incorporated Congou black tea, CTC (crush, tear, and curl), and Souchong black tea. Congou black tea is a traditional full-fermented type of tea in China, which undergoes processing stages including withering, rolling, fermentation (enzymatic oxidation), first drying, and second drying (Liu et al., 2022). Keemun and Yunnan Congou black teas are made from *Camellia sinensis* var. *sinensis* and *Camellia sinensis* var. *assamica*, respectively, and share the same processing technologies with slight modifications in different areas and companies. In our previous investigation, Yunnan Congou black teas exhibited darker red liquor color, higher astringency, and bitter taste intensities than Keemun Congou black tea. Yunnan Congou black teas also had a more significant differential in flavor characteristics including

aroma, color, taste and appearance (Long et al., 2023). These differences may be highly affected by the difference in chemical components and contents in fresh tea leaves.

As suggested in previous studies, the chemical compounds in fresh tea leaves were impacted by the carbon and nitrogen metabolism ratio, which is influenced by altitude (light intensity, light quality, humidity, and temperature), species, and the physiological state (i.e., tree age) of the tea plant, resulting in a change in the proportions of secondary metabolites (Fu et al., 2023; Li et al., 2020). According to the differences in tree ages from which the tea leaves materials were collected, Yunnan Congou black teas were classified into ancient black tea and ordinary black tea. The ancient black tea was manufactured from natural ingredients planted in nonpolluting areas over hundreds of years, usually possessing extreme scarcity, superior qualities, and high commercial values. Therein, the universal definition of the ancient tea tree remains unclear (Wang et al., 2023). The metabolite profile of black teas manufactured by fresh leaves of old-age and young-age tea plants is still ill-defined. Therefore, it is essential to investigate the difference in chemical components and flavor characteristics of black teas from different

\* Corresponding author at: 130 Changjiang West Road, Hefei, Anhui 230036, China.

E-mail address: [zhli2091@sina.com](mailto:zhli2091@sina.com) (L. Zhang).

tree ages.

The sweet-mellow taste and red liquor color are critical factors in evaluating the sensory quality of black tea infusions. Black tea contains various chemical constituents that contribute to the taste and color characteristics, including oxidation products, flavonoid glycosides, amino acids, monosaccharides, and alkaloids (Wang et al., 2023). Several studies have explored that enzymatic oxidation products, such as theaflavins, dihydrotheasinensin, theacitrins, theacitrinins, thearubigins, and theabrownins, were the prominent taste and color components of black tea infusion (Zhou et al., 2022). In recent years, some novel black tea pigments, including epigallocatechin gallate-chlorogenic acid (EGCG-CGA), epigallocatechin-chlorogenic acid (EGC-CGA), and Amadori rearrangement products, were also reported (Wang et al., 2021; Zhang et al., 2018). Previous studies have demonstrated that temperature and time of processing and storage were crucial parameters for taste and color formation in black tea. In contrast, taste contributors, as well as complex yellow and red pigments, changed under different processing conditions (Zhu et al., 2022). These pigments were also reported to form from selective oxidation reactions based on other flavan-3-ol-derived substrates. Thus, black tea's color and taste characteristics were also influenced by the substances of fresh tea leaves picked from different tea plants.

Metabolomic analysis has been widely applied in untargeted and targeted chemical profiles research. Its combination with instrumental analytical tools, such as mass spectrometers (MS), near-infrared spectral (NIR), Raman spectroscopy and nuclear magnetic resonance (NMR) imaging provides a more powerful tool for structural elucidation, as well as plays a crucial role in the authentication, classification, and critical marker substance identification (Chowdhury et al., 2023). With the development of multi-omics technology, comprehensive studies have been conducted on tea samples collected from different varieties, regions, and processing methods (Zhang et al., 2020). Multivariate statistical analysis mainly included unsupervised principal component analysis (PCA) and supervised discriminant or regression analysis. The most commonly used supervised models were partial least squares analysis (PLS) and orthogonal partial least squares analysis (OPLS). These models have been reported as powerful tools for searching key biochemical and flavor compounds and exhibited the most significant differentiating compounds between various samples (Guo et al., 2018).

The present study aims to provide new insight into the metabolite profile and the color and taste contribution of Yunnan Congou black teas with different tree ages through multi-spectral omics combined with sensory evaluation approaches. Based on multivariable statistical analysis, the discriminative metabolites within three types of Yunnan Congou black teas were further screened. These results intended to provide valuable information for exploring and evaluating the crucial flavor-related components of Yunnan Congou black teas. Furthermore, this investigation will advance our understanding of producing high-quality ancient Yunnan Congou black tea in the future.

## 2. Materials and methods

### 2.1. Materials and chemicals

Black tea samples from a thousand years old tea trees (TB), hundreds of years old tea trees (HB), and decades of years tea trees (DB) were supplied by China Tea Liushan (Fengqing) Tea Co., Ltd (Yunnan, China), and the detailed information is listed in Table S1. Fresh tea shoots were harvested from Lincang, Yunnan, China, in the spring of 2022. They were further identified and classified according to the local records of county and expert evaluation. All black tea samples were manufactured through the same Yunnan Congou black tea production process, including withering, rolling, fermentation, and two-step drying. Black tea was sampled three times and thoroughly mixed to obtain a 200 g mixture. Each group of black tea samples was sampled with three repetitions to obtain a total of 600 g samples. The obtained black tea

samples were well labeled and stored at 4 °C till use. Food-grade EGCG, sucrose, and sodium glutamate were purchased from Jushengyuan Biotechnology Company (Xi'an, China). The authentic standards of monosaccharides (>98 %), amino acids (>98 %), and 1-phenyl-3-methyl-5-pyrazolone (>98 %) were purchased from Shanghai Yuanye Biotechnology Company (Shanghai, China). LC-MS grade acetonitrile, methanol, and formic acid were obtained from TEDIA Company Inc. (Fairfield, OH, USA). Potassium dihydrogen phosphate (KH<sub>2</sub>PO<sub>4</sub>, 99.5 %) and phosphoric acid (H<sub>3</sub>PO<sub>4</sub>, 85 %) were purchased from Shanghai Macklin Biochemical Technology Company Limited (Shanghai, China).

### 2.2. Instrumental color analysis

To detect the infusion's color and colorimetric values in CIE Lab/LCH color systems, black tea infusions were prepared referring to the Chinese National Standard (GB/T 23776-2018). These infusions (20 mg/mL) were measured with a 1 cm path length cuvette at immediate temperature and scanned by the colorimeter (CHN SPEC CS-820, Hangzhou, China) at a visible range within 360 to 780 nm (Cui et al., 2022; Long et al., 2023). The illuminant and standard observer were set as D65 and 10°. The Lab and LCH color values were obtained simultaneously. In the Lab color model, the  $L^*$ ,  $a^*$ , and  $b^*$  values represented lightness (0–100), greenness (–100)-redness (+100), and blueness (–100)-yellowness (+100), respectively. In the LCH color model, the  $L^*$ ,  $C^*$ , and  $H^\circ$  values represented lightness (0–100), chroma (0–100), and red (0° and 360°)-yellow (90°)-green (180°)-blue (270°) hue, respectively. In Lab and LCH color models, the  $L^*$  value is the same, while the  $C^*$  and  $H^\circ$  values can be converted by  $a^*$  and  $b^*$  values measured under the same illuminant and standard observer conditions. Then, color images (RGB color system) were illustrated and calculated from Lab/LCH values under identical parameters (D65 illuminant and 10° standard observer). The correlation analysis of colorimetric values was calculated using GGally packages in R software (RStudio, Version R 4.2.2, THU, China).

### 2.3. UV-visible spectra measurements

Ground tea sample (100 mg) was extracted with 4 mL of distilled water, brewed for 5 min, and centrifuged at room temperature at 8000 rpm for 10 min. The samples were extracted three times. Following centrifugation, the supernatant was mixed and diluted to 10 mL with distilled water. The UV-visible absorbance spectra of black tea infusions were recorded within the range of visible spectra 360–780 nm (same visible spectral range as colorimeter mentioned in section 2.2) with PerkinElmer Lambda 35 UV-visible spectrometer (Waltham, MA, USA). The optimum dilution was performed to accomplish an absorbance range between 0.2 and 0.8 for all black tea infusions.

### 2.4. Equivalent quantification of tea taste quality

Food-grade EGCG, sucrose, and sodium glutamate were used as taste standards. The gradient concentrations and corresponding points are presented in Table S2. The black tea infusions were prepared to refer to GB/T 23776-2018 and evaluated at room temperature regarding the taste intensity by ten trained tea panelists (five men and five women). A 9-cm line scale (10-point scale) was used for sensory evaluation to score the taste attributes. The scores were determined based on the ruler-measured distance between the left end and the panelists' markers (Cao et al., 2019; Huang et al., 2021).

### 2.5. Quantitative analysis of main compounds

The samples were extracted with distilled water, as described in section 2.3, to avoid the effects of different pH on tea infusions' color and chemical characteristics. The quantitative analysis of catechins, purine alkaloids, gallic acid (GA), theaflavins, monosaccharides, and amino acids was conducted according to the method published (Wen et al.,

2021). The levels of catechins, purine alkaloids, GA and theaflavins, and monosaccharides were carried out using ultra-high performance liquid chromatography system (UHPLC Infinity 1290 and Infinity 1260, Agilent Technologies, Santa Clara, CA, USA) coupled to a diode array detector (DAD) and were separated on ACQUITY UPLC BEH Shield RP18 column ( $2.1 \times 50$  mm,  $1.7 \mu\text{m}$ ) and Agilent TC-C<sub>18</sub> column ( $4.6 \times 250$  mm,  $5 \mu\text{m}$ ). The mobile phases applied to determine catechins, purine alkaloids, GA, and theaflavins were acetonitrile–water (containing 0.1 % formic acid), and gradient elution was set as follows: 0–2.5 min, 2 % B; 2.5–3 min, 2–5 % B; 3–8 min, 5–15 % B; 8–14 min, 15–30 % B; 14–16 min, 30–50 % B; 16–18 min, 50–2 % B; 18–22 min, 2 % B. The mobile phase applied to determine monosaccharides was water (containing 0.60 % KH<sub>2</sub>PO<sub>4</sub>-0.50 % triethylamine buffer)-acetonitrile and gradient elution was set as follows: 0–6 min, 84 % A; 6–8 min, 84–78 % A; 8–25 min, 78–75 % A; 25–27 min, 75–73 % A; 27–32 min, 73–84 % A. The settings of UHPLC and DAD were as follows: the detection wavelengths at 278 nm and 250 nm, the injection volumes at 1  $\mu\text{L}$  and 5  $\mu\text{L}$ , the flow rates at 0.90 mL/min and 0.25 mL/min, the column ovens at 40 °C and 35 °C. The concentrations of amino acids were analyzed using the ExionLC system (AB Sciex) coupled to a triple-quadrupole (QQQ) mass spectrometer (API 5500 QTRAP™ MS/MS system from AB Sciex, Concord, ON, Canada). They were separated on the Comixshell CARP column ( $150 \times 4.6$  mm,  $2.7 \mu\text{m}$ ). The mobile phases were water (containing 0.1 % formic acid)-acetonitrile (containing 5 % water and 0.05 % formic acid) and gradient elution was set as follows: 0–2 min, 2 % B; 2–17 min, 2–100 % B; 17–19 min, 100 % B; 19–21 min, 100–2 % B; 21–25 min, 2 % B. The settings of UHPLC and QQQ were as follows: the injection volume at 5  $\mu\text{L}$ , the flow rate at 1 mL/min, and the column oven at 35 °C. The content of thearubigins and theabrownins was quantified by the spectrophotometry method (NY/T 3675–2020) (Cui et al., 2022). The detection wavelength was set at 380 nm. Every experiment was carried out three times. The dose-over-threshold (Dot) factors were calculated as the concentration ratio (mol/L) and the reported taste threshold in the literature.

## 2.6. Identification of color and taste-related metabolites by untargeted metabolomics by UHPLC-Q-TOF-MS

The samples were extracted with water as described in section 2.3 and analyzed by ultra-high performance liquid chromatography tandem quadrupole time-of-flight mass spectrometry (UHPLC-Q-TOF-MS) (Agilent Technologies, USA) using the method reported (Long et al., 2023). Chromatographic separation was achieved using an ACQUITY UPLC BEH Shield RP18 column ( $2.1 \times 50$  mm,  $1.7 \mu\text{m}$ ) with a gradient elution composed of eluents A (0.1 % formic acid water) and eluents B (100 % acetonitrile) at a flow rate of 0.3 mL/min. The column's temperature was set at 35 °C, and the injection volume of the extract was 2  $\mu\text{L}$ . The gradient elution was set as follows: 0–5 min, 98 % A; 5–15 min, 95–85 % A; 15–17 min, 85–79 % A; 17–19 min, 50–2 % A; 19–21 min, 2 % A; 21–23 min, 2–98 % A; 23–25 min, 98 % A. The UHPLC-Q-TOF-MS data were processed, including deconvolution and alignment, by MS-DIAL software and further analyzed using Simca-P 14.0 software (Umetrics AB, Umea, Sweden). The PCA and OPLS regression models were analyzed using Simca-P 14.0 software. The color and taste values were set as *Y* variables (dependent variables), while the alignment peak area was specified as *X* variables (predictor variables).

## 2.6. Regression and correlation analysis of metabolites and color and taste values

The OPLS regression models were further analyzed using Simca-P 14.0 software. The variable influence on projection (VIP) > 2 compounds were set as *X* variables, and the color and taste values were set as *Y* variables, respectively. The color and taste values of the black tea in this OPLS regression model were calculated as Eq. (1.1)

$$Y(\text{value}) = Y(\text{average}) + X_1B_1 + \dots + X_nB_n \quad (1.1)$$

The *Y*(value) indicated the evaluated colorimetric values and taste scores, which were inputted as the *Y* variables in the OPLS models. The *Y* (average) represents the mean value of all *Y* values for all samples in the model. The *B* values (regression coefficients) were computed to express how strongly *Y* correlates to each *X*-variable. The *n* values represented the number of *X* variables. Therein, the error bars indicated the confidence intervals of the coefficients of each metabolite. The coefficients were regarded as significant ( $P < 0.05$ ), considering the confidence interval excludes zero (Guo et al., 2018).

The Pearson correlation coefficients of chromatic value and metabolites were calculated and illustrated using the psych and corplot packages in R software. The correlation matrix of metabolites with strong correlation ( $r > 0.8$  and  $< -0.8$ ) was uploaded to the Gephi software (Version: 0.10.1), and then the Fruchterman–Reingold algorithm was used for network visualization analysis.

## 2.7. Statistical analysis

Each reaction and sample treatment were operated in triplicates. The results were expressed as mean value  $\pm$  standard deviation (SD) from IBM SPSS Statistics 27 (IBM, Armonk, NY, USA). The data were analyzed using one-way analysis of variance (ANOVA), and the statistical difference between the three treatments was determined at  $P < 0.05$  using Fisher's least significant difference (LSD) and Duncan methods.

## 3. Results and discussion

### 3.1. The effects of tree age on color and taste characteristics of black teas

#### 3.1.1. Colorimetric values and UV-visible spectra

To observe the color characteristics of black tea infusions, sensory evaluation, colorimeter, and UV-visible spectrophotometry analysis were performed, respectively. The infusions were extracted with water according to GB/T 23776-2018, which is also capable of conducting sensory evaluation. Fig. 1A and B demonstrated that DB, HB, and TB samples presented significantly distinct color features. The TB infusion showed the lowest level of saturation (lowest  $C^*$  value) and deeper yellow hue (highest  $H^*$  value) compared to DB and HB samples (Fig. 1C). In addition, the HB infusion showed the deepest red hue (lowest  $H^*$  value) and darkest in terms of brightness (lowest  $L^*$  value), corresponding to the results of sensory evaluation (Fig. 1A). In addition, TB samples exhibited the highest  $H^*$  value, indicating that TB presented a deeper yellow hue by human visualization than DB and HB samples. However, the TB sample had the lowest  $b^*$  value, representing the lowest level of yellowness in the Lab color system. These results agreed with our previous study that a high  $b^*$  value in the Lab color model does not represent a yellow tea infusion observed by human eyes (Long et al., 2023). That might be explained by the high content of red pigments, such as catechins oxidation products, masked the yellow hue and resulted in a red hue appearance of tea infusions.

Herein, correlation analysis has been used to explain the interdependency relationships for Lab ( $L^*$ ,  $a^*$  and  $b^*$ ) and LCH ( $L^*$ ,  $C^*$  and  $H^*$ ) color values, and detailed results are illustrated in Fig. S2. The results showed that  $a^*$  and  $b^*$  values significantly correlated negatively with the brightness of black tea infusion, indicating that colored substances had a higher visible absorption capacity and reduced the brightness of tea infusions.

Three black tea infusions exhibited similar absorbance curves within the range of visible spectrum 360–780 nm, of which absorbance ranging 360–450 nm presented yellow by human visualization (Fig. S1). The absorbance values gradually decreased within the 450–780 nm wavelength range of UV-visible spectra. These results suggested that the main chromophore-containing compounds of three black teas were similar

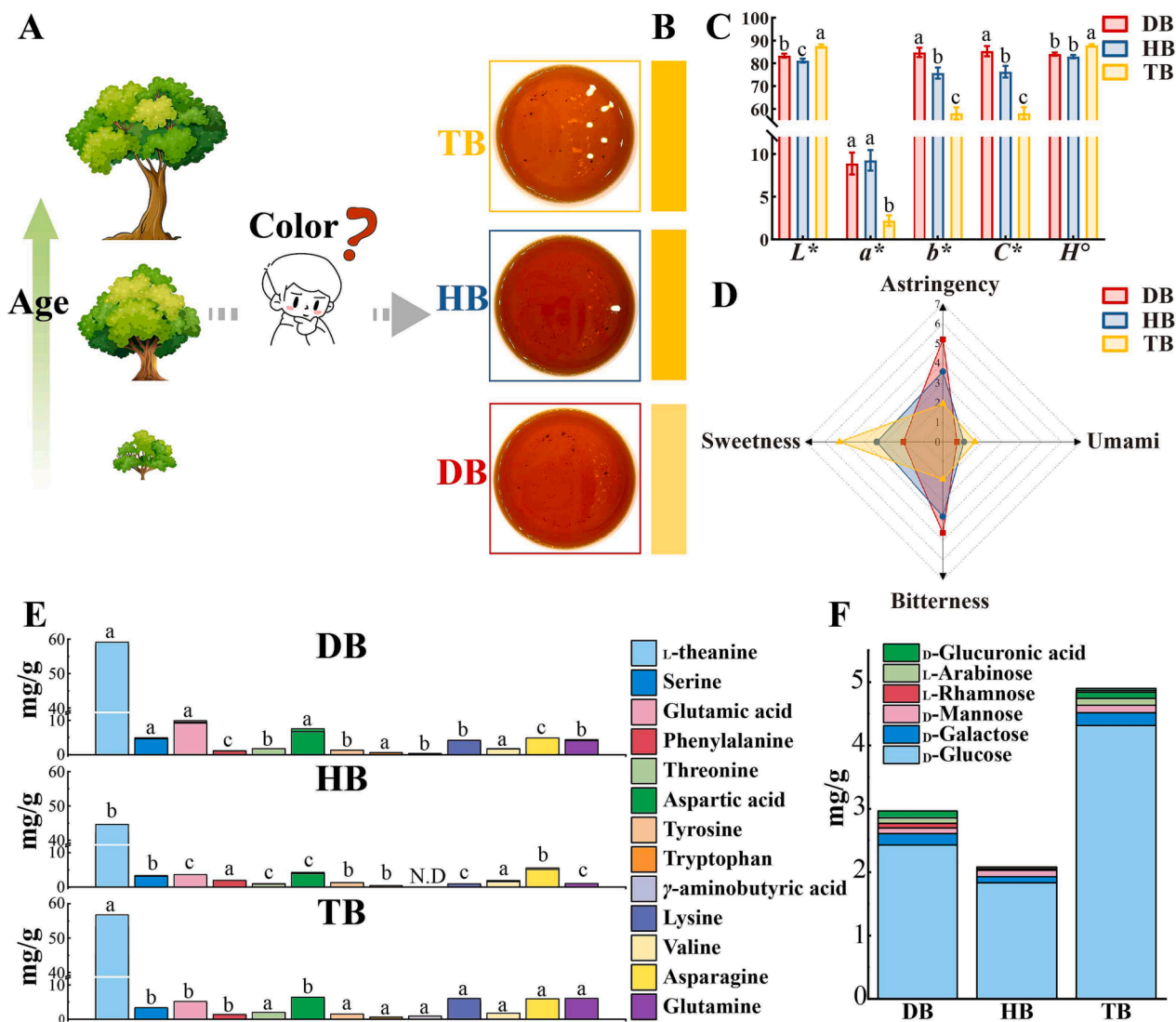


**Fig. 1.** Color, taste and chemical characteristics of different ages black tea samples. Color appearances (A), RGB color images (B), and colorimetric values (C) of black tea infusions. (D) Four taste evaluations of black tea infusions. The amino acids (E) and free monosaccharides (F) content in black tea infusions. Different superscript lowercase letters (a, b, c) indicate a significant difference ( $P < 0.05$ ).

but with minor changes in the quantitative results.

### 3.1.2. Taste of black tea samples

All black tea infusions were compared by sensory evaluation of quantitative descriptive analysis (10-point scale) regarding the umami, sweetness, astringency and bitterness tastes. The taste scores of DB, HB, and TB samples are shown in Fig. 1D. Results showed that with the increase of tree age, the umami and sweetness scores of black tea infusion increased significantly, but the astringency and bitterness scores decreased. TB infusion presented significantly lower bitterness and astringency scores but had apparent sweet and umami characteristics while appearing with a sweet-mellow sensation. DB and HB infusions exhibited higher bitterness and astringency scores than TB. Tea infusion taste was formed from the synthetic perception of various taste-active compounds, such as polyphenols and amino acids.

## 3.2. Chemical characterization of black tea

### 3.2.1. Catechins, caffeine, theobromine, and tea pigments

The content of the main non-volatile compounds in black tea infusions was determined to quantitatively depict the differences in color and taste. It has been widely reported that black tea contains low levels

of catechins, such as EGCG, galocatechin gallate (GCG), and epicatechin gallate (ECG), the primary taste components in green tea. These components were mostly converted to thearubigins and theabrownins during fermentation (enzymatic oxidation) stage and their levels were lower in black tea. Tables 1 and S3 showed the levels of catechins, caffeine, GA, theobromine, and corresponding Dot factor in DB, HB, and TB. With increasing tree age, the content of catechins (EGCG, GCG, ECG), GA, theobromine, and caffeine decreased significantly. For example, in comparison to the HB and TB samples, the DB sample contained a much higher concentration of ECG and caffeine, contributing to the astringency and bitterness of tea infusion (Table S3).

Theaflavins, thearubigins and theabrownins are important pigments in black tea. Tables 1 and S3 showed that the Dot factors of theaflavin-3-gallate (TF2a) were below 1, which means they do not contribute to astringency sensation in DB, HB, and TB samples. The average level of theabrownins was the highest in DB (66.65 mg/g), followed by HB (44.55 mg/g) and TB (35.30 mg/g), while that of thearubigins showed the opposite trend, 75.12 mg/g in DB, 78.93 mg/g in HB and 86.98 mg/g in TB. The theabrownins content could indicate the transformation of thearubigins during the fermentation stage. In addition, theabrownins have been reported to be responsible for the color and taste formation of black and dark teas (Long et al., 2023). Higher content of catechins may

**Table 1**  
The concentrations of main compounds in Yunnan Congou black tea samples.

Compounds (mg/g)	DB	HB	TB
EGCG	0.02 ± 0.02 <sup>a</sup>	N.D.	N.D.
GCG	0.75 ± 0.06 <sup>a</sup>	N.D.	N.D.
ECG	5.79 ± 0.20 <sup>a</sup>	1.48 ± 0.08 <sup>b</sup>	1.18 ± 0.10 <sup>c</sup>
GA	5.12 ± 0.31 <sup>a</sup>	1.78 ± 0.18 <sup>b</sup>	1.70 ± 0.03 <sup>b</sup>
THB	6.43 ± 0.34 <sup>a</sup>	1.64 ± 0.03 <sup>b</sup>	0.84 ± 0.02 <sup>c</sup>
CAF	26.48 ± 1.31 <sup>a</sup>	24.00 ± 0.40 <sup>b</sup>	21.56 ± 0.52 <sup>c</sup>
TF2a	0.49 ± 0.20 <sup>a</sup>	0.41 ± 0.01 <sup>a</sup>	0.49 ± 0.01 <sup>a</sup>
TF3	N.D.	N.D.	0.43 ± 0.01 <sup>a</sup>
TRs	75.12 ± 2.00 <sup>b</sup>	78.93 ± 2.48 <sup>b</sup>	86.98 ± 2.59 <sup>a</sup>
TBs	66.65 ± 4.21 <sup>a</sup>	44.55 ± 1.44 <sup>b</sup>	35.30 ± 2.98 <sup>c</sup>

Note: The results were presented as mean ± SD of three independent experiments; different superscript lowercase letters (a, b, c) indicate significant differences ( $P < 0.05$ ); N.D. means not detected. EGCG: epigallocatechin gallate, GCG: galocatechin gallate, ECG: epicatechin gallate, GA: gallic acid, THB: theobromine, CAF: caffeine, TF2a: theaflavin-3-gallate, TF3: theaflavin 3,3'-digallate, TRs: thearubigins, TBs: theabrownins.

lead to the increased formation of thearubigins in DB and TB and subsequently induce the accumulation of theabrownins.

### 3.2.2. Amino acids

Amino acids are crucial flavor substances in tea, which play essential roles in umami and sweet tastes and participate in forming aroma and color during manufacturing. Thirteen free amino acids were quantitatively determined, such as the main umami-related theanine, glutamine, glutamic acid, asparagine and aspartic acid. Results showed that DB and TB samples contained a higher content of amino acids, as described in Fig. 1E. It was reported that the amino acids content in fresh leaves is age-dependent and can be easily modulated via plant management practice, cultivation environment, and processing method (Chen et al., 2021). Under high-altitude conditions such as in Yunnan province, differential light and temperature have been reported to increase the free amino acid content while decreasing the levels of polyphenols in fresh tea leaves (Wang et al., 2022). A similar variation was found in ancient tea plantations (>100 years) and modern tea plantations (<60 years), of which the former contained a higher content of free amino acids (Yang et al., 2022). Furthermore, researchers have reported that the contents of amino acids significantly decreased during the drying stage, possibly due to participation in non-enzymatic reactions (Yu et al., 2021). The content of amino acids was lower in the HB sample, possibly due to their degradation during two following drying processes and the formation of the highest level of red hue and darkest lightness (Fig. 1A).

Among 13 amino acids, theanine was the predominant umami amino acid, and its content was 42.10 to 58.53 mg/g in three black tea samples according to the quantitative analysis by LC-QQQ-MS. The content of theanine was the highest in the TB sample, but theanine was incapable of providing direct umami sensation due to its content being below the threshold value (Table S3).  $\gamma$ -Aminobutyric acid (GABA) has mouth coating and mouth-drying sensation and has a lower recognition threshold of 20  $\mu\text{mol/L}$  (Rotzoll et al., 2005). Lower levels of GABA were only observed in DB and TB samples and showed a higher Dot factor than 2, possibly contributing to the astringency taste of tea infusions. These findings revealed that, among 13 amino acids, solely GABA contributes to the taste perception of DB, HB, and TB.

### 3.2.3. Free monosaccharides

The concentrations of 9 free monosaccharides were compared through HPLC analysis with previously published method (Wen et al., 2021). Six free monosaccharides were detected, of which  $\text{D}$ -glucose was the main free monosaccharide with a level of 1.78 to 4.25 mg/g. It has been reported as important and essential taste-active compound contributing to the sweetness of tea infusion. The TB sample had the highest level of total free monosaccharides, including  $\text{D}$ -glucose (Fig. 1F).

Nevertheless, the concentrations of  $\text{D}$ -glucose were below the sweetness threshold, lending little power to sweet sensation in DB, HB, and TB samples (Table S3).

Monosaccharides can undergo Maillard reactions with amino acids to produce a series of thermal reaction products during the high-temperature drying process of black tea, contributing to the color and taste of tea infusion. Compared to TB and DB samples, HB had a lowest total concentration of monosaccharides and amino acids, suggesting that the color of HB infusion may be attributed to Maillard reaction during high-temperature processing (Fig. 1E and F). Therefore, these results indicated that the concentration of the main color compounds of black tea with different tree ages had significant differences.

### 3.3. Determination of key color and taste-related compounds of different ages of black tea

#### 3.3.1. The multivariate analysis results of LC-MS-based metabolomics

To investigate the color and taste metabolites in black tea infusion further, a multivariate statistical analysis method was performed using UHPLC-Q-TOF-MS. After pretreatment of the UHPLC-Q-TOF-MS data, 6756 metabolites with their mass information were detected after the alignment of DB, HB, and TB datasets. As illustrated in Fig. 2A, the PCA analysis and QC samples were employed to validate the repeatability and stability of the sample preparation and instrumental analysis. PCA scatter plot showed a tight clustering on QC tea samples and was situated close to the coordinate origin, which validated excellent data analyzability.

Furthermore, the hierarchical clustering analysis (HCA) result demonstrated that HB and TB samples were grouped, suggesting their similar chemical profiling (Fig. 2B). The Venn diagram was calculated from their metabolites resulting from alignment data to reveal the difference in the number of metabolites. Fig. 2F showed that most metabolites were identical in the three black tea samples.

The supervised OPLS regression models have been applied to identify the importance of metabolites with color and taste. The colorimeter values plus absorbance values ( $L^*$ ,  $a^*$ ,  $b^*$ ,  $C^*$ ,  $H^*$  and 360–780 nm visible spectra) and taste scores (umami, sweetness, astringency, bitterness) were set as Y variables in color OPLS model and taste OPLS model, respectively (Long et al., 2023). The  $Q^2$  values of color and taste OPLS regression models were close to 1 (0.934 and 0.997, respectively), providing a solid color and taste value predictability. The results of permutation tests of color and taste regression models were exhibited in Table S4, with all  $R^2$  values below 0.4 and  $Q^2$  values below 0.05 in the validated model. These results confirmed the stability and suitability of these models.

Examining the scatter plots of the color and taste models, the DB, HB, and TB samples are divided into three sections based on the Y value trend (Fig. 2C and E). The loading plots of supervised color and taste OPLS models were used to investigate the most differential metabolites among three black teas. The size and color of each metabolite represented the VIP values and average peak area of three black teas in the individual OPLS model. Some metabolites, including EC, quercetin 3-O-rutinoside, and *trans*-4-O-*p*-coumaroylquinic acid, were in the same quadrant of color and taste loading plots, suggesting these metabolites were critical compounds for distinguishing color and taste values of three black tea infusions (Fig. 2D and E). These results indicated that the significant differential compounds among the three types of black tea were involved in determining the color and taste of black tea. Finally, 84 compounds (VIP > 2) were selected and identified as crucial color and taste-related metabolites. Their VIP values in color and taste OPLS models are shown in Table 2.

#### 3.3.2. Key color and taste-related metabolites of black teas from the different tree age

Most key color and taste compounds were retrieved and determined by literature, authentic standards, fragment structure and tea

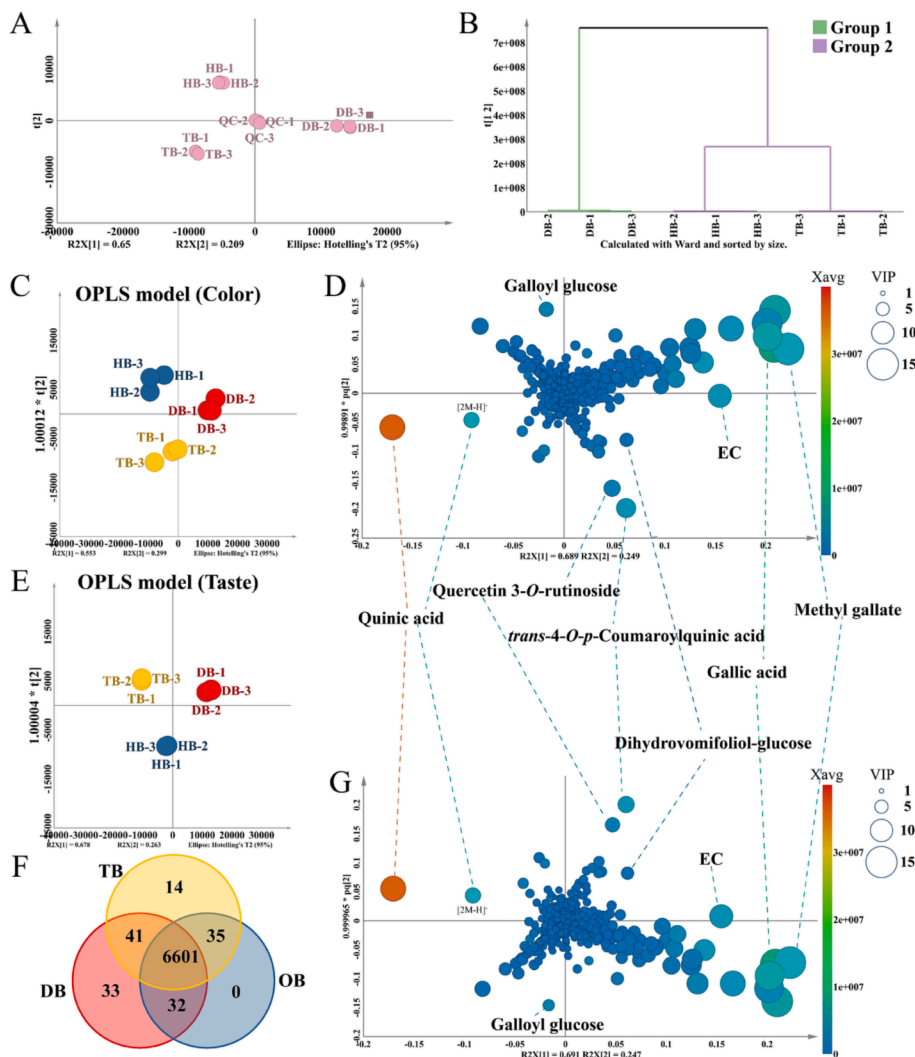


**Fig. 2.** Multivariate statistical analysis reveals the main differential compounds of Yunnan Congou black tea samples in different tree ages. A: PCA scatter plot of black tea samples and QC samples. B: The HCA diagram of DB, HB, and TB samples. Scatter plot and loading plot of OPLS model of color (C and D) and OPLS model of taste (E and G) of different ages black tea samples. F: A Venn diagram showing the overlap of metabolites in DB, HB, and TB samples.

metabolome database (TMDB) combined with retention time, and further details can be found in Table 2. Eighty-four key color and taste-related metabolites, including Amadori rearrangement products, triterpenoid saponins, amino acids, catechin oxidation products, organic acids, and flavonol glycosides. Flavone glycosides were tentatively identified, and the VIP values of color and taste model and MS/MS fragment ion were also listed in Table 2. The quantitative heat map with a standardized Z-score was applied to identify the most differential metabolites in DB, HB, and TB samples (Fig. S4). Eighty-four key flavor-related compounds exhibited different patterns. Hydrolysable tannins, catechin oxidation products, catechins, organic acids, flavonol glycosides, and flavone glycosides were the main differential substances in DB, HB, and TB samples. The Venn diagram displayed in Fig. S3 showed that the VIP compounds in color and taste models were mostly the same, demonstrating that crucial color and taste-related metabolites simultaneously affect the color and taste of black tea infusions.

### 3.3.3. Correlation and regression analyses results between color and taste-related metabolites

Based on the multivariate statistical analysis of multi-spectral omics data, some critical metabolites have been proposed, which were responsible for distinguishing three black tea samples with different tree ages. To analyze the dependency relationship between individual

metabolites and the color and taste of black tea samples the correlation of all metabolites, a full-correlation network of metabolites, color, and taste was successfully profiled by SPSS and Gephi. The visualization of compound-compound, and compound-color/taste with correlation coefficients ranging from 0.8 to 1.0 and  $-1.0$  to  $-0.8$  was achieved in Fig. 3A. The font size of each metabolite was calculated according to the number of metabolites it significantly correlated with. The results suggested a strong correlation between different metabolites' content, colorimetric values, and taste scores.

To verify the effectiveness of 84 key metabolites on color and taste, two concise OPLS regression models were rebuilt using these metabolites' mass data as an X variable. In contrast, color parameters (360–780 nm visible spectra and colorimetric values) combined with taste value were designated as a Y variable. The fitting  $Q^2$  value was 0.997 and 0.956 for taste and color, respectively, indicating good prediction based on these key metabolites. The regression coefficient of each metabolite regarding color and taste parameters was calculated as Equation (1.1) and shown in Fig. 3B, which represents the impact on color and taste scores.

**3.3.3.1. Catechins and their derivatives.** Catechins and their oxidation products, such as theogallin and theasinensins, were selected as vital color- and taste-related metabolites. A total of 8 oxidation products were

**Table 2**  
The key color and taste-related compounds contributing to the color and taste of Yunnan Congou black tea samples.

RT (min)	<i>m/z</i>	Compounds	MS/MS	VIP (color)	VIP (taste)
0.594	333.068	Dehydro theanine-glucose Amadori product	155.082, 173.093, 241.012	2.490	2.930
0.480	132.033	<i>L</i> -Aspartic acid	99.927, 115.922	3.100	3.020
0.532	173.095	Theanine	155.083	3.030	2.790
3.132	387.135	Dihydrovomifoliol-glucose	179.073	3.930	4.610
6.384	635.096	Trigalloyl glucose	169.013, 313.055, 465.066, 483.077	8.470	8.320
1.034	331.071	Galloyl glucose-1	169.015, 271.049	4.470	3.940
1.221	331.071	Galloyl glucose-2	169.016, 271.049	5.000	4.820
1.493	331.071	Galloyl glucose-3	129.977, 169.015	4.360	4.330
3.067	483.080	Digalloyl glucose-1	125.026, 169.017, 313.059	2.850	3.300
3.403	483.084	Digalloyl glucose-2	125.026, 169.016, 271.049, 423.061	4.310	4.300
3.821	483.083	Digalloyl glucose-3	125.026, 169.016, 313.060, 423.061	4.870	4.840
4.223	483.084	Digalloyl glucose-4	125.026, 169.016, 271.018, 313.058, 423.097	5.930	5.870
7.954	463.072	Galloyl-xylopyranosyl-glucopyranoside	125.026, 169.016, 293.047, 311.057	7.070	7.090
0.815	481.068	Unknown-1	211.003, 301.000, 362.054	5.390	4.990
3.003	633.078	Galloyl-HHDP-glucose-1	275.022, 301.005, 463.056	2.050	2.340
3.874	633.079	Galloyl-HHDP-glucose-2	191.057, 301.000, 463.048	2.160	2.460
4.495	633.080	Galloyl-HHDP-glucose-3	301.003, 463.055	9.440	8.860
4.001	289.075	C	109.029, 125.024, 203.071, 245.082	5.900	6.260
4.808	289.076	EC	109.031, 125.026, 245.085	9.270	10.090
3.633	305.071	EGC	102.957, 125.026, 263.022	4.300	4.180
7.953	441.088	ECG	169.016, 289.075	13.360	13.320
6.070	457.081	EGCG	125.026, 169.016, 307.844	7.400	7.040
10.436	425.093	Epiafzelechin gallate	169.016, 255.069, 273.079, 359.848	3.040	2.770
7.963	439.069	Epicatechin gallate quinone	125.026, 169.016, 289.073	4.100	3.780
6.086	455.065	3'- <i>O</i> -Methyl(-)-epicatechin 3- <i>O</i> -gallate	125.026, 169.016	3.280	3.180
4.483	577.139	Procyanidin B1	289.078, 375.072	2.270	2.290
5.190	577.141	Procyanidin B2	125.025, 161.026, 245.084, 289.073, 407.082	5.780	5.500
2.141	609.132	Unknown-2	112.988, 202.940, 473.863	2.970	2.750
5.223	761.144	Procyanidin dimer (EGCG-EGC)	125.014, 218.087, 262.077, 530.034, 625.117	4.880	4.720
4.620	799.148	Theogallin	437.056, 455.065, 485.040	2.880	2.790
7.190	913.158	Theasinensin A or D	125.026, 435.076, 573.107, 591.120, 743.130	3.700	3.640
7.600	301.003	Ellagic acid	185.026, 284.002	4.400	3.930
11.510	447.097	Quercetin 3- <i>O</i> -rhamnoside	271.027, 300.030	5.420	6.280
9.048	463.095	Quercetin 3- <i>O</i> -glucoside	271.028, 300.031	3.910	2.810
8.816	463.092	Quercetin 3- <i>O</i> -galactoside	271.028, 300.031	3.920	4.520
8.166	609.154	Quercetin 3- <i>O</i> -robinobioside	151.004, 300.028	3.060	2.530
8.455	609.156	Quercetin 3- <i>O</i> -rutinoside	300.031	5.290	5.330
10.137	609.152	Quercetin 3- <i>O</i> -glucoside 7- <i>O</i> -rhamnoside	300.031	2.310	2.670
16.736	901.253	Quercetin-rhamnopyranosyl-glucopyranosyl-rhamnopyranosyl-rhamnopyranoside or isomer	271.017, 301.034, 447.091, 755.181	2.880	2.920
11.000	447.099	Kaempferol 3- <i>O</i> -glucoside	227.035, 255.028, 284.032	5.240	4.130
10.239	447.097	Kaempferol 3- <i>O</i> -galactoside	227.037, 255.032, 284.036, 327.052	3.460	3.910
10.358	593.159	Kaempferol 3- <i>O</i> -robinobioside	285.044	7.410	7.230
10.358	661.146	Kaempferol 3- <i>O</i> -robinobioside derivative	231.625, 285.040, 593.159	3.120	3.050
14.721	431.101	Kaempferol 3- <i>O</i> -rhamnoside	227.039, 255.032, 285.043	2.080	2.400
17.925	739.175	Kaempferol-di- <i>p</i> -coumaroyl-glucopyranoside or isomer	145.029, 285.039, 352.399, 453.116, 593.127	1.900	2.080
6.534	739.212	Kaempferol-rhamnopyranosyl-glucopyranosyl-rhamnopyranoside or isomer-1	285.039, 593.154	1.840	2.140
9.910	739.218	Kaempferol-rhamnopyranosyl-glucopyranosyl-rhamnopyranoside or isomer-2	285.044, 463.085, 593.154	5.650	5.610
9.332	755.213	Kaempferol-glucopyranosyl-rhamnopyranosyl-glucopyranoside or isomer-2	285.043	2.380	2.650
8.130	755.213	Kaempferol-glucopyranosyl-rhamnopyranosyl-glucopyranoside or isomer-1	285.043, 300.030	2.190	2.450
13.138	781.221	Kaempferol 3-glycoside	169.012, 442.864, 481.529, 631.762	2.020	1.980
16.882	871.235	Kaempferol-di- <i>p</i> -coumaroyl-xylopyranosyl-glucopyranoside	145.024, 169.012, 285.038	2.630	3.010
16.786	885.257	Kaempferol-tri- <i>p</i> -coumaroyl-glucopyranoside or isomer	145.030, 285.038, 431.097, 574.169, 739.184	2.520	2.680
16.721	1017.300	Kaempferol-tri- <i>p</i> -coumaroyl-arabinosyl-glucopyranoside or isomer	285.036, 431.093, 497.073, 725.198, 871.228	2.160	2.480
6.779	533.137	Apigenin 6-8-di- <i>C</i> -arabinopyranoside	383.082, 443.102, 515.0019	2.000	2.110
5.807	563.148	Apigenin 6- <i>C</i> -arabinoside 8- <i>C</i> -glucoside	353.071, 383.081, 443.105, 473.114, 503.124	2.020	1.920
9.282	593.155	Vitexin 2'- <i>O</i> - $\beta$ - <i>D</i> -glucoside	284.035	2.410	2.790
6.935	593.155	Isovitexin 7- <i>O</i> -glucoside	285.042, 431.101, 447.096, 473.033	1.780	2.060
6.334	785.089	Chakaflavonoid B	61.990, 301.001, 553.20, 760.086	2.540	2.900
0.599	133.017	Malic acid	71.015, 75.010, 89.027, 115.005	1.840	2.090
7.211	137.027	Salicylic acid	65.041, 93.036	2.220	2.360
1.395	169.017	Gallic acid	125.026	13.440	13.640
4.135	179.037	Caffeic acid	135.047	2.180	2.220
0.535	191.063	Quinic acid	85.031	10.850	11.150
0.475	311.104	Xylopyranosyl-glucopyranose	179.054	2.170	2.490

(continued on next page)

Table 2 (continued)

RT (min)	m/z	Compounds	MS/MS	VIP (color)	VIP (taste)
5.645	337.097	<i>cis</i> -5- <i>O</i> - <i>p</i> -Coumaroylquinic acid	173.047, 191.058	2.880	3.330
5.092	337.098	<i>trans</i> -4- <i>O</i> - <i>p</i> -Coumaroylquinic acid	119.052, 163.041, 173.048, 191.058	6.460	6.600
5.472	337.098	<i>trans</i> -5- <i>O</i> - <i>p</i> -Coumaroylquinic acid	93.035, 119.052, 191.058	1.930	2.180
1.714	343.072	Theogallin (3-Galloylquinic acid)	191.059	14.600	14.000
4.370	353.091	5- <i>O</i> -Caffeoylquinic acid	191.059	2.380	2.570
4.135	353.092	4- <i>O</i> -Caffeoylquinic acid	135.047, 173.048, 179.037, 191.059	6.500	6.590
8.610	489.109	Galloyl-coumaroyl-quinic acid	173.047, 337.096	2.810	2.800
0.910	513.058	Quinic acid rhamnosyl-glucuronide	191.037, 235.027, 277.038, 337.060, 365.054	2.890	2.230
11.508	515.084	Quercetin 3- <i>O</i> -rhamnoside derivative	284.037, 447.098	2.050	2.380
4.851	135.048	4'-Hydroxyacetophenone	93.036	2.420	2.810
5.534	177.022	5,7-Dihydroxycoumarin	65.004, 89.041, 133.031	2.570	2.910
3.158	183.031	Methyl gallate	78.011, 124.019, 168.006	14.250	14.550
0.501	195.055	Unknown-3	59.014, 75.009, 99.009	4.190	3.190
1.250	344.045	cGMP	133.015, 150.042, 190.995	3.180	2.860
3.069	411.029	Gallic acid derivative	96.961, 169.016, 241.005	2.970	3.260
0.910	305.023	Unknown-4	111.021	2.260	2.210
0.813	579.037	Quinic acid derivative	191.018	3.230	2.990
16.978	467.198	Unknown-5	129.975, 313.069, 401.086	2.450	2.410
17.818	1173.580	Chakasaponin IV	903.483, 993.509	7.360	8.530
17.882	1215.590	Unknown-6	–	2.390	2.760

detected and selected in our study (Table 2 and Fig. 3). Catechin monomers and dimers presented similar decreasing trends when tea tree age was increased. Heatmap analysis was applied to illustrate the variation of these metabolites in DB, HB, and TB samples, and the DB sample showed the highest amount of oxidation products (Fig. S4). These results indicated that the DB sample contained a higher amount of catechins in fresh tea leaves than HB and TB, then correspondingly produced more oxidation products, such as theasinensin A/D, theogallin, theaflavins, thearubigins and theabrownins.

Catechins and their oxidation products are important taste contributors in black tea, and their taste properties are bitter and astringent (Zhang et al., 2020). The correlation analysis results illustrated that all catechins and oxidation products had a significantly positive relationship with bitterness and astringency scores in black tea samples (Fig. S6). The DB contained higher concentrations of catechins and oxidation products, correspondingly showed stronger astringent and bitter tastes (Fig. 1D). In recent years, the quality attribute of catechins such as astringency and bitterness have been widely reported, among which EGCG, EGC, and ECG have been illustrated to have astringency and bitterness taste (Xu et al., 2018). Overall, the higher content of catechins and their oxidation products was detected in tea produced from the youngest tea trees (DB sample), corresponding to a more bitter and astringent taste and darker color.

**3.3.3.2. Flavonoid glycosides and their derivatives.** Flavonoid glycosides have been reported to have lower astringent taste threshold than catechins and also had inhibition effects on the sweet-mellow taste in tea infusion (Li et al., 2019). Furthermore, flavonoid glycosides contribute significantly to the formation of the yellow hue and lightness of tea infusion due to the absorption band in the visible light range of about 360–380 nm (Agati et al., 2011; Zhang et al., 2018). Among 84 key color and taste-related compounds, 28 flavonoid glycosides and derivatives were identified, suggesting that different tree age black teas reflected significant differences in flavonoid glycosides.

Heatmap analysis (Fig. S4) confirmed the variations between DB, HB, and TB samples. TB possessed the most varied and highest total levels of flavonoid glycosides, followed by DB and HB. Therein, Quercetin 3-*O*-glucoside 7-*O*-rhamnoside, Kaempferol-rhamnopyranosyl-glucopyranosyl-rhamnopyranoside or isomer, isovitexin 7-*O*-glucoside, chakaflavonoid B and chakasaponin IV were only detected in HB. Chakasaponin IV has been reported to be widely distributed in tea flowers, but they were first detected in black tea as a VIP compound (Shen et al., 2017; Zhang et al., 2018). Likewise, the HB sample had the

highest content of apigenin glycosides, including apigenin 6–8-di-*C*-arabinopyranoside and apigenin 6-*C*-arabinoside 8-*C*-glucoside (Table 2 and Fig. S4). These results might be attributed to special cultivation environment, altitude and temperature of 600–1000 years tea trees.

In contrast, Kaempferol-di-*p*-coumaroyl-glucopyranoside or isomer, Kaempferol-glucopyranosyl-rhamnopyranosyl-glucopyranoside or isomer, kaempferol 3-glycoside and apigenin 6–8-di-*C*-arabinopyranoside were not detected in TB, of which kaempferol 3-glycoside was only detected in DB. In addition, quercetin 3-*O*-rhamnoside and kaempferol 3-*O*-rhamnoside solely occurred in HB and TB samples, and their levels in TB were significantly higher than HB, reaching 37.99 and 72.17-fold. In contrast, DB sample had the highest mass intensity of kaempferol 3-*O*-robinobioside, followed by HB and TB samples. Other flavonoid glycosides, including kaempferol 3-*O*-robinobioside, Kaempferol-rhamnopyranosyl-glucopyranosyl-rhamnopyranoside or isomer-2, Kaempferol-glucopyranosyl-rhamnopyranosyl-glucopyranoside or isomer-2 and vitexin 2'-*O*- $\beta$ -*D*-glucoside, also increased or decreased conspicuously in their contents with increasing tree age. These data agreed with previous studies that tea cultivars and the environment quantitatively and qualitatively affected the flavonoid glycosides of tea (Shi et al., 2021). Flavonols, flavones, and their glycosides were secondary metabolites widely distributed in tea plants and presented in fresh tea shoots, buds, and leaves. They significantly decreased by hydrolysis and thermal reactions during black tea processing. Fig. 3A and B results showed that quercetin 3-*O*-rutinoside had a significant positive relationship with bitter and astringent tastes, which was discovered to have a mild astringent taste and enhance the bitterness of EGCG (Chen et al., 2022). Therefore, the highest bitter and astringent scores of DB might be attributed to the interaction of EGCG and quercetin 3-*O*-rutinoside. Accordingly, these results implied that tea plants of different ages possessed varying types and levels of flavonols, flavones, and glycosides in fresh leaves, resulting in various flavor characteristics after the same processing method, suggesting that these flavonoid glycosides were tree age specificity.

As described above, the HB had lower total levels of flavonoid glycosides, amino acids, and free monosaccharides than DB and TB samples (Figs. 2 and S4). Additionally, the HB sample had the lowest  $L^*$  and  $H^*$  values, representing a redder hue and observable darker shade (Fig. 1A and B). Fermentation oxidation and Maillard reaction were critical reactions involving black tea infusion color formation. However, the HB sample exhibited lower levels of thearubigins and theabrownins than DB sample, which did not show deeper color. These results implied that the Maillard reaction might be highly involved during the processing of the



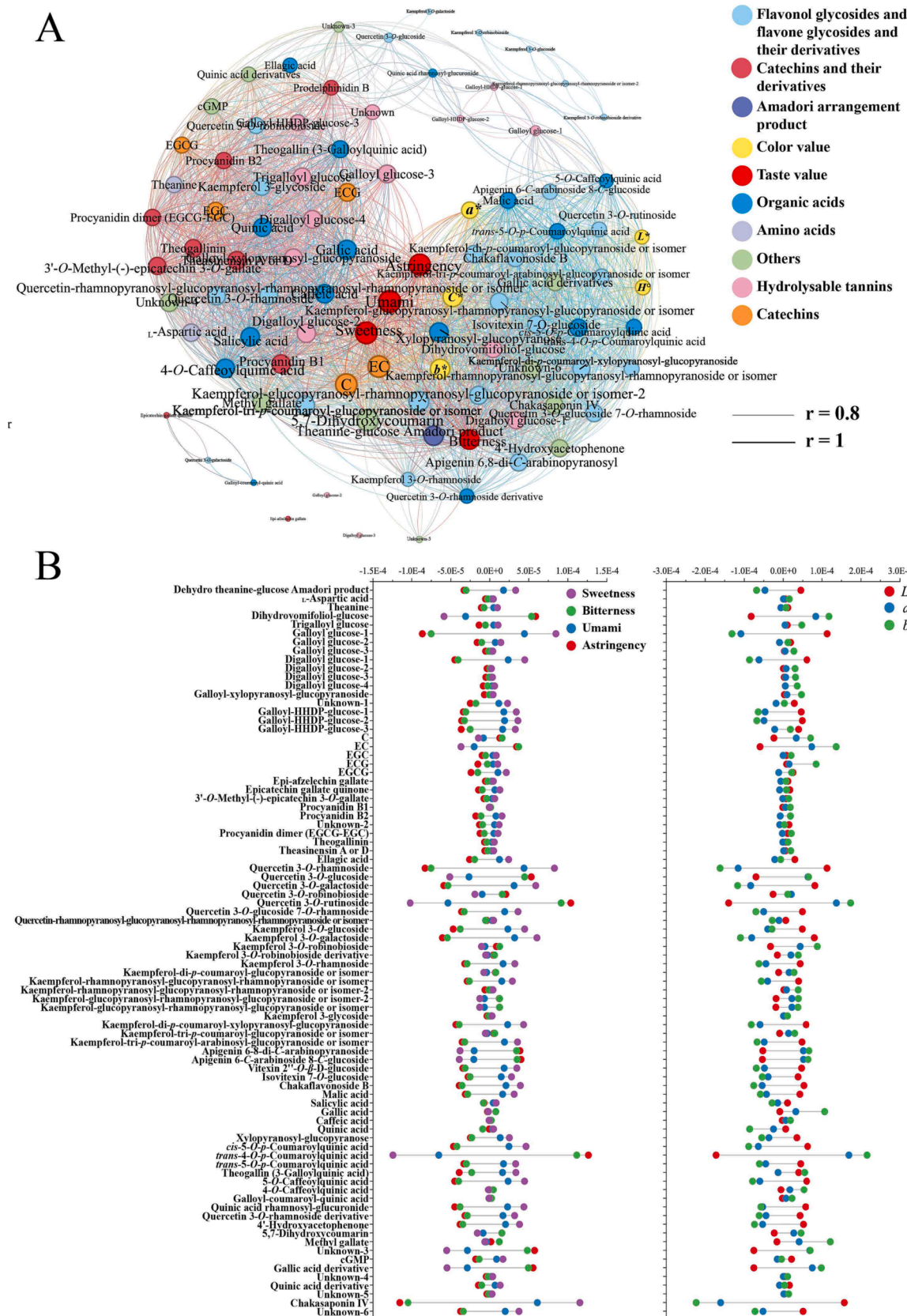


Fig. 3. A: Network diagram demonstrating the correlation between crucial color and taste-related compounds and colorimetric and taste values in DB, HB, and TB samples. B: Regression coefficients of 84 key color and taste-related compounds in taste and color OPLS regression models.

HB sample, resulting in the formation of darker-colored melanoidin-like substances.

**3.3.3.3. Organic acids.** Organic acids identified included quinic acid, GA, salicylic acid, coumaroylquinic acids and caffeoylquinic acids in black tea samples, all of which were reported as taste compounds or modifiers (Cao et al., 2019; Kaneko et al., 2006). Our interest in researching quinic acid herein is that it is an effective taste substance with enhanced effects, including sourness and umami (Hutasingh et al., 2023). The highest level of quinic acid was detected in three black tea infusions within 16 organic acid substances. TB sample showed the highest levels of quinic acid, followed by HB and DB samples. Enriched quinic acid in the TB sample may enhance the umami taste of L-theanine and other amino acids.

Similarly, the previous study recognized theogallin and GA as umami-enhancing and sweet aftertaste substances (Cao et al., 2019; Wang et al., 2021). Our results revealed that the DB sample had a higher content of GA, caffeic acid, theogallin, and 4-O-caffeoylquinic acid than the HB and TB samples (Fig. S4). However, the contributions of these

compounds may be lower than bitter and astringency components in the DB sample, and their taste-enhancing effects were covered. As seen in Fig. 3B, *trans*-4-*O*-*p*-coumaroylquinic acid had the highest regression coefficient with bitter and astringency values than others, which was consistent with the results reported by Wen et al., who identified *trans*-4-*O*-*p*-coumaroylquinic acid as the astringency contributing compound in Keemun black tea (Wen et al., 2022).

An increasing body of evidence suggests that organic acids containing acidic groups are important color modifiers by regulating the pH value of tea infusions (Yu et al., 2022; Zhang et al., 2023). The pH values of DB, HB, and TB samples were measured within the range of 4.85–4.90, as displayed in Fig. S5. A previous study showed that the acidic conditions enabled higher chroma (higher  $a^*$  and  $b^*$  values) and lower lightness than alkaline conditions in black tea infusions. In addition, tea infusions with lower pH values promoted to have lower  $a^*$  and  $b^*$  values while having higher lightness values (Han et al., 2022). The results indicated that these organic acids were important taste and color modifiers in Yunnan Congou black tea infusions.

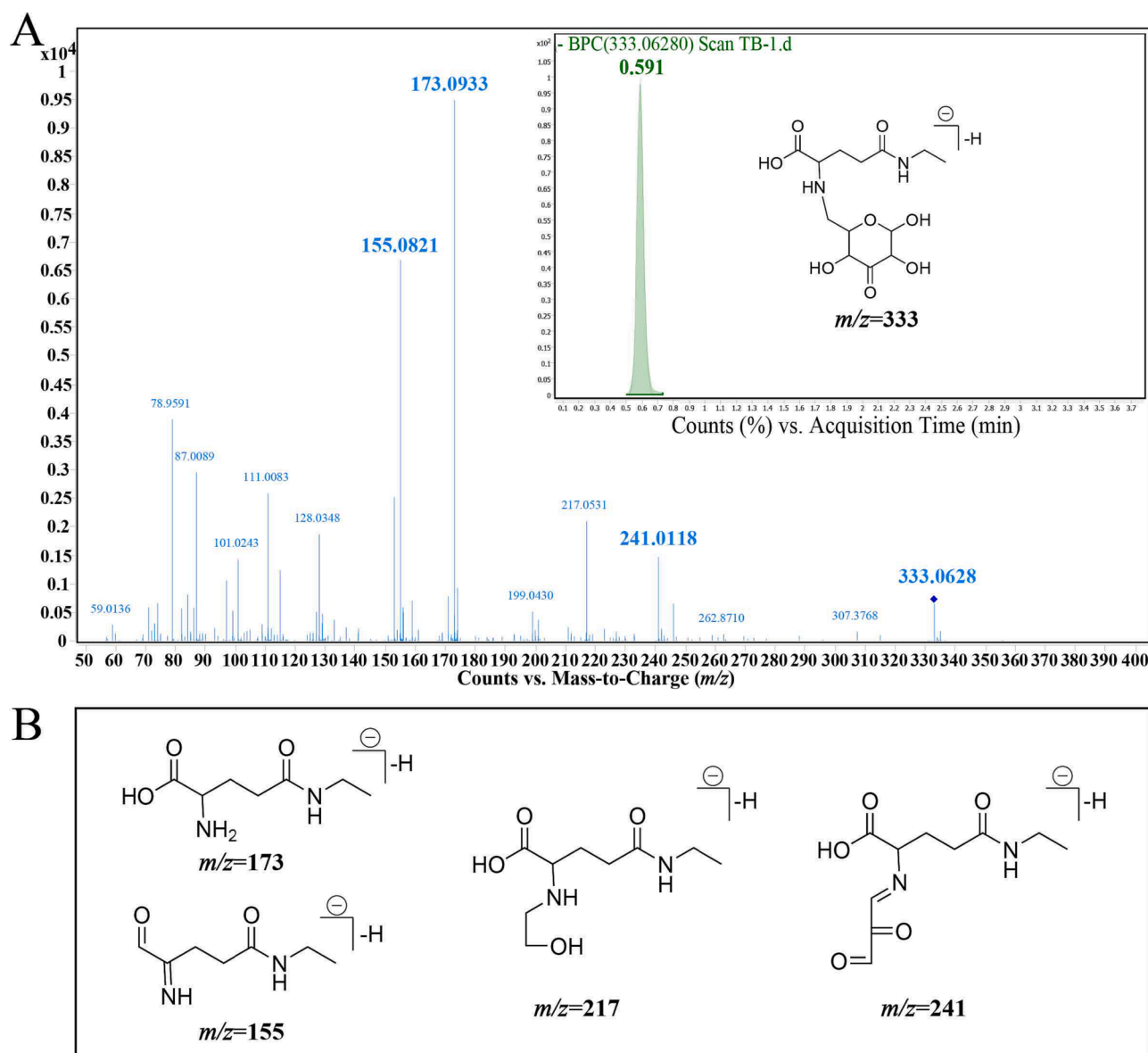


**Fig. 4.** UHPLC-Q-TOF-MS analysis of dehydro theanine-glucose Amadori product. A: Mass spectrum and secondary mass spectra of dehydro theanine-glucose Amadori product. B: Fragmentation pathways and proposed structure of dehydro theanine-glucose Amadori product ( $m/z = 333$ ).

**3.3.3.4. Analysis of Amadori products.** Thermal products occurred with the Maillard reaction, and degradation and polymerization play an integral role in tea flavor and gained more validation results through simulated reactions and experiments. Among the 84 key color and taste-related compounds, most of the oxidation products, flavonoids, and organic acids were widely studied. In the present study, a novel Amadori rearrangement product that occurred in the initial stage of the Maillard reaction was tentatively identified, with a negative ion at  $m/z$  333 exhibiting higher VIP values in two OPLS models. Its VIP values in color and taste OPLS models were 2.490 and 2.930, which reflected more contribution to color and taste (Table 2).

The ESI-MS results suggested that it has a molecular ion peak around 0.591 min at  $m/z$  333.0628 under negative ionic mode (Fig. 4A). To pinpoint the chemical structure of this novel component, the corresponding MS/MS fragment ions were inspected. Among detected results,  $m/z$  173, 155, 217 and 241 were detected and suggested containing theanine and glucose moiety (Fig. 4B). In the previous study, Han et al. isolated and identified two Amadori rearrangement products, the theanine-glucose Amadori product (ARP 1) and pyroglutamic acid-glucose Amadori product (ARP 2), derived from the thermal model reaction system of theanine and glucose (Han et al., 2022). In this study, ARP 1 and ARP 2 were detected by LC-MS, and identical retention time and fragment ions were shown for the important VIP compound at  $m/z$  333. Therefore, this compound was tentatively identified as a dehydro theanine-glucose Amadori product. The proposed plane structure and main fragmentation pathway of  $m/z$  333 are shown in Fig. 4.

Furthermore, using further correlation analysis, the dehydro theanine-glucose Amadori product exhibited significant positive correlation and regression coefficients with umami and sweetness scores (Fig. S6). The content of this Amadori product was determined to be the highest in HB, followed by HB and DB samples (Fig. S4). Amadori rearrangement product occurred in the initial Maillard reaction and accounts for flavor formation during the thermal processing of tea. In addition, it has been reported to possess umami-enhancing properties (Wang et al., 2021). The results implied this essential compound could have potential umami and sweet taste or taste-enhancing properties. Besides, this compound was speculated to contain nitrogen atoms, C=O, and C=N bonds, indicative of appearing pale and deep yellow with increasing concentrations. A previous study has also reported that the proline-glucose Amadori product presents a yellow hue (Wang et al., 2021). Therefore, we speculated that the dehydro theanine-glucose Amadori product possibly enhanced the umami and sweet intensities and yellow hue of black tea infusions.

#### 4. Conclusion

Multi-spectral omics combined with a sensory evaluation approach were applied to analyze color and taste compounds from abundant metabolites to distinguish Yunnan Congou black teas from tea plants with ages of decades to a thousand years. Eighty-four critical color and taste-related metabolites were selected and tentatively identified, including Amadori rearrangement product, catechin oxidation products, flavonol glycosides, flavone glycosides, and organic acids, which suggested that variation in these components are critical for color and taste characteristics. The levels and types of flavonoid glycosides and organic acids showed tree age specificity. The black tea from a thousand years tea tree was observed to possess a high content of theanine, glucose and dehydro theanine-glucose Amadori product. In contrast, the lower content of catechins, enzymatic oxidation products, *trans*-4-O-p-coumaroylquinic acid, and quercetin 3-O-rutinoside were probably responsible for the superior taste quality and emerging sweet-mellow perception. Our results specifically suggested that detecting unique metabolites such as chakasaponin IV was an ideal strategy to distinguish black teas from tea trees of different ages. These findings comprehensively investigated the color and taste properties and related contribution constituents of Yunnan Congou black tea produced with different

tea plants from decades to a thousand years. It will provide valuable information to explore, determine, and evaluate the key color and taste-related metabolites in Yunnan Congou black teas. However, further extraction, separation, and sensory studies are needed to assess the effects of novel metabolites on the color and taste contribution of high-quality black tea.

#### Ethical approval

Participants gave informed consent via the statement, "I am aware that my responses are confidential, and I agree to participate in this survey," where an affirmative reply was required to enter the survey. They could withdraw from the survey at any time without giving a reason. The products tested were safe for consumption.

#### CRediT authorship contribution statement

**Piaopiao Long:** Writing – original draft, Visualization, Data curation, Conceptualization. **Shengxiao Su:** Writing – review & editing, Data curation. **Zisheng Han:** Writing – review & editing, Resources. **Daniel Granato:** Conceptualization, Writing – review & editing. **Wei Hu:** Writing – review & editing, Data curation. **Jiaping Ke:** Writing – review & editing. **Liang Zhang:** Writing – review & editing, Supervision, Funding acquisition, Conceptualization.

#### Declaration of competing interest

The authors declare that they have no known competing financial interests or personal relationships that could have appeared to influence the work reported in this paper.

#### Data availability

Data will be made available on request.

#### Acknowledgments

This work was supported by the excellent scientific research and innovation team of Anhui Province for Universities (2023AH010027), National Natural Science Foundation of China (32122079, 32072633), and earmarked fund for CARS-19.

#### Appendix A. Supplementary data

Supplementary data to this article can be found online at <https://doi.org/10.1016/j.fochx.2024.101190>.

#### References

- Agati, G., Cerovic, Z. G., Pinelli, P., & Tattini, M. (2011). Light-induced accumulation of ortho-dihydroxylated flavonoids as non-destructively monitored by chlorophyll fluorescence excitation techniques. *Environmental and Experimental Botany*, 73, 3–9. <https://doi.org/10.1016/j.envexpbot.2010.10.002>
- Cao, Q. Q., Zou, C., Zhang, Y. H., Du, Q. Z., Yin, J. F., Shi, J., Xue, S., & Xu, Y. Q. (2019). Improving the taste of autumn green tea with tannase. *Food Chemistry*, 277, 432–437. <https://doi.org/10.1016/j.foodchem.2018.10.146>
- Chen, Y., Zhou, B., Li, J., Tang, H., Zeng, L., Chen, Q., Cui, Y., Liu, J., & Tang, J. (2021). Effects of long-term non-pruning on main quality constituents in 'Dancong' Tea (*Camellia sinensis*) leaves based on proteomics and metabolomics analysis. *Foods*, 10 (11). <https://doi.org/10.3390/foods10112649>
- Chen, Y. H., Zhang, Y. H., Chen, G. S., Yin, J. F., Chen, J. X., Wang, F., & Xu, Y. Q. (2022). Effects of phenolic acids and quercetin-3-O-rutinoside on the bitterness and astringency of green tea infusion. *npj Science of Food*, 6(1), 8. <https://doi.org/10.1038/s41538-022-00124-8>
- Chowdhury, C. R., Kavitha, D., Jaiswal, K. K., Jaiswal, K. S., Reddy, G. B., Agarwal, V., & Shetty, P. H. (2023). NMR-based metabolomics as a significant tool for human nutritional research and health applications. *Food Bioscience*, 53, Article 102538. <https://doi.org/10.1016/j.fbio.2023.102538>
- Cui, Y., Lai, G., Wen, M., Han, Z., & Zhang, L. (2022). Identification of low-molecular-weight color contributors of black tea infusion by metabolomics analysis based on

- UV-visible spectroscopy and mass spectrometry. *Food Chemistry*, 386, Article 132788. <https://doi.org/10.1016/j.foodchem.2022.132788>
- Fu, Z., Chen, L., Zhou, S., Hong, Y., Zhang, X., & Chen, H. (2023). Analysis of differences in the accumulation of tea compounds under various processing techniques, geographical origins, and harvesting seasons. *Food Chemistry*, 430, Article 137000. <https://doi.org/10.1016/j.foodchem.2023.137000>
- Guo, X., Long, P., Meng, Q., Ho, C.-T., & Zhang, L. (2018). An emerging strategy for evaluating the grades of Keemun black tea by combinatory liquid chromatography-Orbitrap mass spectrometry-based untargeted metabolomics and inhibition effects on  $\alpha$ -glucosidase and  $\alpha$ -amylase. *Food Chemistry*, 246, 74–81. <https://doi.org/10.1016/j.foodchem.2017.10.148>
- Han, H., Wang, H., Gao, G., Rao, P., Zhou, J., Ke, L., & Xu, Y. (2022). pH effect on colloidal characteristics of micro-nano particles in lapsang souchong black tea infusion. *Food Control*, 133, 10864. <https://doi.org/10.1016/j.foodcont.2021.108643>
- Han, Z., Jiang, Z., Zhang, H., Qin, C., Rong, X., Lai, G., Wen, M., Zhang, L., Wan, X., & Ho, C.-T. (2022). Amadori reaction products of theanine and glucose: Formation, structure, and analysis in tea. *Journal of Agricultural and Food Chemistry*, 70(37), 11727–11737. <https://doi.org/10.1021/acs.jafc.2c04560>
- Huang, A., Jiang, Z., Tao, M., Wen, M., Xiao, Z., Zhang, L., Zha, M., Chen, J., Liu, Z., & Zhang, L. (2021). Targeted and nontargeted metabolomics analysis for determining the effect of storage time on the metabolites and taste quality of keemun black tea. *Food Chemistry*, 359, Article 129950. <https://doi.org/10.1016/j.foodchem.2021.129950>
- Hutasingh, N., Chuntakaruk, H., Tubtimrattana, A., Ketngamkum, Y., Pewlong, P., Phaonakrop, N., Roytrakul, S., Rungrotmongkol, T., Paemane, A., Tansrisawad, N., Siripatrawan, U., & Sirikantaramas, S. (2023). Metabolite profiling and identification of novel umami compounds in the chaya leaves of two species using multiplatform metabolomics. *Food Chemistry*, 404(Pt A), Article 134564. <https://doi.org/10.1016/j.foodchem.2022.134564>
- Kamiloglu, S., Tomas, M., Ozdal, T., & Capanoglu, E. (2021). Effect of food matrix on the content and bioavailability of flavonoids. *Trends in Food Science & Technology*, 117, 15–33. <https://doi.org/10.1016/j.tifs.2020.10.030>
- Kaneko, S., Kumazawa, K., Masuda, H., Henze, A., & Hofmann, T. (2006). Molecular and sensory studies on the umami taste of Japanese green tea. *Journal of Agricultural and Food Chemistry*, 54(7), 2688–2694. <https://doi.org/10.1021/jf0525232>
- Li, J., Yao, Y., Wang, J., Hua, J., Wang, J., Yang, Y., Dong, C., Zhou, Q., Jiang, Y., Deng, Y., & Yuan, H. (2019). Rutin,  $\gamma$ -aminobutyric acid, gallic acid, and caffeine negatively affect the sweet-mellow taste of Congou black tea infusions. *Molecules*, 24(23). <https://doi.org/10.3390/molecules24234221>
- Li, Y., Jeyaraj, A., Yu, H., Wang, Y., Ma, Q., Chen, X., Sun, H., Zhang, H., Ding, Z., & Li, X. (2020). Metabolic regulation profiling of carbon and nitrogen in tea plants [*Camellia sinensis* (L.) O. Kuntze] in response to shading. *Journal of Agricultural and Food Chemistry*, 68(4), 961–974. <https://doi.org/10.1021/acs.jafc.9b05858>
- Liu, F., Wang, Y., Corke, H., & Zhu, H. (2022). Dynamic changes in flavonoids content during Congou black tea processing. *Lwt-Food Science and Technology*, 170, Article 114073. <https://doi.org/10.1016/j.lwt.2022.114073>
- Long, P., Li, Y., Han, Z., Zhu, M., Zhai, X., Jiang, Z., Wen, M., Ho, C.-T., & Zhang, L. (2023). Discovery of color compounds: Integrated multispectral omics on exploring critical colorant compounds of black tea infusion. *Food Chemistry*, 432, Article 137185. <https://doi.org/10.1016/j.foodchem.2023.137185>
- Long, P., Rakariyatham, K., Ho, C.-T., & Zhang, L. (2023). Thearubigins: Formation, structure, health benefit and sensory property. *Trends in Food Science & Technology*, 133, 37–48. <https://doi.org/10.1016/j.tifs.2023.01.013>
- Rotzoll, N., Dunkel, A., & Hofmann, T. (2005). Activity-guided identification of (S)-malic acid 1-O-D-glucopyranoside (morelid) and gamma-aminobutyric acid as contributors to umami taste and mouth-drying oral sensation of morel mushrooms (*Morchella deliciosa* Fr.). *Journal of Agricultural and Food Chemistry*, 53(10), 4149–4156. <https://doi.org/10.1021/jf050056i>
- Shen, X., Shi, L., Pan, H., Li, B., Wu, Y., & Tu, Y. (2017). Identification of triterpenoid saponins in flowers of four *Camellia Sinensis* cultivars from Zhejiang province: Differences between cultivars, developmental stages, and tissues. *Industrial Crops and Products*, 95, 140–147. <https://doi.org/10.1016/j.indcrop.2016.10.008>
- Shi, J., Yang, G., You, Q., & Lv, H. (2021). Updates on the chemistry, processing characteristics, and utilization of tea flavonoids in last two decades (2001–2021). *Critical Reviews in Food Science and Nutrition*, 63(20), 4747–4784. <https://doi.org/10.1080/10408398.2021.2007353>
- Wang, F., Cheng, X., Cheng, S., Li, W., & Huang, X. (2023). Genetic diversity of the wild ancient tea tree (*Camellia taliensis*) populations at different altitudes in Qianjianghai. *PLoS One*, 18(4), e0283189.
- Wang, H., Cao, X., Yuan, Z., & Guo, G. (2021). Untargeted metabolomics coupled with chemometrics approach for Xinyang Maojian green tea with cultivar, elevation and processing variations. *Food Chemistry*, 352, Article 129359. <https://doi.org/10.1016/j.foodchem.2021.129359>
- Wang, M., Yang, J., Li, J., Zhou, X., Xiao, Y., Liao, Y., Tang, J., Dong, F., & Zeng, L. (2022). Effects of temperature and light on quality-related metabolites in tea [*Camellia sinensis* (L.) Kuntze] leaves. *Food Research International*, 161, Article 111882. <https://doi.org/10.1016/j.foodres.2022.111882>
- Wang, Y., Cui, H., Zhang, Q., Hayat, K., Yu, J., Hussain, S., Tahir, M. U., Zhang, X., & Ho, C.-T. (2021). Proline-glucose Amadori compounds: Aqueous preparation, characterization and saltiness enhancement. *Food Research International*, 144, Article 110319. <https://doi.org/10.1016/j.foodres.2021.110319>
- Wen, M., Cui, Y., Dong, C.-X., & Zhang, L. (2021). Quantitative changes in monosaccharides of Keemun black tea and qualitative analysis of theaflavins-glucose adducts during processing. *Food Research International*, 148, Article 110588. <https://doi.org/10.1016/j.foodres.2021.110588>
- Wen, M., Han, Z., Cui, Y., Ho, C.-T., Wan, X., & Zhang, L. (2022). Identification of 4-O-p-coumaroylquinic acid as astringent compound of Keemun black tea by efficient integrated approaches of mass spectrometry, turbidity analysis and sensory evaluation. *Food Chemistry*, 368, Article 130803. <https://doi.org/10.1016/j.foodchem.2021.130803>
- Xu, Y. Q., Zhang, Y. N., Chen, J. X., Wang, F., Du, Q. Z., & Yin, J. F. (2018). Quantitative analyses of the bitterness and astringency of catechins from green tea. *Food Chemistry*, 258, 16–24. <https://doi.org/10.1016/j.foodchem.2018.03.042>
- Yang, G., Zhou, D., Wan, R., Wang, C., Xie, J., Ma, C., & Li, Y. (2022). HPLC and high-throughput sequencing revealed higher tea-leaves quality, soil fertility and microbial community diversity in ancient tea plantations: Compared with modern tea plantations. *BMC Plant Biology*, 22(1), 239. <https://doi.org/10.1186/s12870-022-03633-6>
- Yu, F., Chen, C., Chen, S., Wang, K., Huang, H., Wu, Y., He, P., Tu, Y., & Li, B. (2022). Dynamic changes and mechanisms of organic acids during black tea manufacturing process. *Food Control*, 132, Article 108535. <https://doi.org/10.1016/j.foodcont.2021.108535>
- Yu, P., Huang, H., Zhao, X., Zhong, N., & Zheng, H. (2021). Dynamic variation of amino acid content during black tea processing: A review. *Food Reviews International*, Article 2015374. <https://doi.org/10.1080/87559129.2021.2015374>
- Zhang, C., Wang, M., Gao, X., Zhou, F., & Shen, C. (2020a). Multi-omics research in albino tea plants: Past, present, and future. *Scientia Horticulturae*, 261, Article 108943. <https://doi.org/10.1016/j.scienta.2019.108943>
- Zhang, L., Cao, Q.-Q., Granato, D., Xu, Y.-Q., & Ho, C.-T. (2020b). Association between chemistry and taste of tea: A review. *Trends in Food Science & Technology*, 101(1), 139–149. <https://doi.org/10.1016/j.tifs.2020.05.015>
- Zhang, L., Liu, Y., Wang, Y., Xu, M., & Hu, X. (2018a). UV-Vis spectroscopy combined with chemometric study on the interactions of three dietary flavonoids with copper ions. *Food Chemistry*, 263, 208–215. <https://doi.org/10.1016/j.foodchem.2018.05.009>
- Zhang, S., Li, Q., Wen, S., Sun, L., Chen, R., Zhang, Z., Cao, J., Lai, Z., Li, Z., Lai, X., Wu, P., Sun, S., & Chen, Z. (2023). Metabolomics reveals the effects of different storage times on the acidity quality and metabolites of large-leaf black tea. *Food Chemistry*, 426, Article 136601. <https://doi.org/10.1016/j.foodchem.2023.136601>
- Zhang, S., Yang, C., Idehen, E., Shi, L., Lv, L., & Sang, S. (2018b). Novel theaflavin-type chlorogenic acid derivatives identified in black tea. *Journal of Agricultural and Food Chemistry*, 66(13), 3402–3407. <https://doi.org/10.1021/acs.jafc.7b06044>
- Zhou, J., Fang, T., Li, W., Jiang, Z., Zhou, T., Zhang, L., & Yu, Y. (2022). Widely targeted metabolomics using UPLC-QTRAP-MS/MS reveals chemical changes during the processing of black tea from the cultivar *Camellia sinensis* (L.) O. Kuntze cv. Huangjinya. *Food Research International*, 162(Pt B), Article 112169. <https://doi.org/10.1016/j.foodres.2022.112169>
- Zhu, J., Wang, J., Yuan, H., Ouyang, W., Li, J., Hua, J., & Jiang, Y. (2022). Effects of fermentation temperature and time on the color attributes and tea pigments of Yunnan Congou black tea. *Foods*, 11(13), 1845. <https://doi.org/10.3390/foods11131845>
- Zhu, M.-Z., Li, N., Zhou, F., Ouyang, J., Lu, D.-M., Xu, W., Li, J., Lin, H.-Y., Zhang, Z., Xiao, J.-B., Wang, K.-B., Huang, J.-A., Liu, Z.-H., & Wu, J.-L. (2020). Microbial bioconversion of the chemical components in dark tea. *Food Chemistry*, 312, Article 126043. <https://doi.org/10.1016/j.foodchem.2019.126043>